

A NAVAL PERSPECTIVE ON SHIP STABILITY

Arthur M. Reed, Carderock Division, Naval Surface Warfare Center, arthur.reed@navy.mil

ABSTRACT

From a naval perspective, three areas have been identified as critical for examining the performance of vessels in extreme seas: the physics of large-amplitude motions; verification, validation and accreditation (VV&A) of tools for these conditions; and performance-based criteria. In the physics of large-amplitude motions, three topics are most important: hydrodynamic forces, maneuvering in waves, and large-amplitude roll damping. In the VV&A arena, the challenge remains for performing this function for extreme seas conditions, where linear concepts such as response amplitude operators are not applicable. The challenge of performance-based criteria results from the fact that it is on the leading edge of our knowledge base.

Keywords: *Physics of Large-amplitude Motions; Verification, Validation and Accreditation (VV&A); Performance-based Criteria*

1. INTRODUCTION

A navy has the same concerns relative to stability failures that all ship owners, designers and operators have. The significant differences arise from the fact that a navy is not governed by IMO regulations; that the naval vessel is often much more costly than a commercial vessel; and that the naval vessel may not have the luxury of avoiding dangerous weather conditions when performing its missions, while a commercial vessel may be able to choose an alternate route. In addition to these differences, a navy often has access to more research and development funds to investigate these issues than the commercial builder and operator.

As a consequence of the above, the US Navy has been conducting extensive research on the physics of stability failures; investigating the processes by which computational tools for predicting stability failures can be verified, validated, and accredited (VV&A'd) for use in certifying the dynamic behavior of vessels; and developing performance-based stability criteria. In the physics of large-amplitude motions, three

topics have been identified as most important: hydrodynamic forces, maneuvering in waves, and large-amplitude roll damping. In the VV&A arena, performing this function for extreme seas conditions, where linear concepts such as response amplitude operators are not applicable, continues to be a challenge. The challenge of performance-based criteria results from the fact that it is on the leading edge of our knowledge base and therefore, treading paths that have previously been unexplored.

This paper is divided into three major sections, each of which provides an introduction to, and hopefully some insight into, the three areas mentioned above from a naval perspective: physics of large-amplitude motions, VV&A of tools for predicting stability failures, and performance-based criteria.

2. PHYSICS OF LARGE-AMPLITUDE MOTIONS

In order to obtain insight into the behavior of naval vessels in extreme seas, the US Navy

has performed many experiments in extreme seas and has also performed computations corresponding to the experimental conditions. Comparisons of the experiments and computations have shown a number of discrepancies, particularly in following and stern-quartering seas, where the frequency of encounter is low.

Examination of the differences between the experiments and predictions has identified several possible deficiencies in our understanding of the physics of large-amplitude motions. These include the hydrodynamic forces, the modeling of maneuvering in waves, and time-domain roll damping for large roll angles. The three following subsections will discuss what we have learned, and are currently doing, in these three areas.

2.1 Hydrodynamic Forces

Traditionally, the modeling of large-amplitude motions in extreme seas has relied on the use of what we call blended methods — methods that employ a combination of linear and nonlinear computations to compute the fluid forces on the vessel (Beck & Reed, 2001). Typically, this means that the hydrostatic restoring forces and the Froude-Krylov (incident wave) exciting forces are calculated fully nonlinearly; and that the radiation (corresponding to linear added-mass and damping) and diffraction forces are calculated linearly.

To determine if the blended method assumptions are correct and to develop an understanding of the forces on a vessel undergoing large-amplitude motions, a numerical experiment was performed using a variety of computational tools. These computational tools ranged from linear to blended to fully nonlinear. The complete experiment is documented in a massive report, Telste & Belknap (2008); Belknap & Telste

(2008) contains a more complete summary than is included herein.

Vessels Selected. For this investigation, two hulls representative of contemporary naval combatant hull forms were chosen. The first was NSWCCD Models 5415 & 5514, the preliminary design hull form for the DDG 51 class (Hayden, et al., 2006). The other was the tumble-home version of the hull forms in the ONR Topside Series. These were used to investigate the effect of topside shape on motions, as the topside varied from flared to wall-sided to tumblehome with the same underwater form across the 3 variants (Bishop, et al, 2005). The body plans of the two hulls investigated are shown in Figure 1, and the full-scale particulars, for which the force predictions were made, are shown in Table 1.

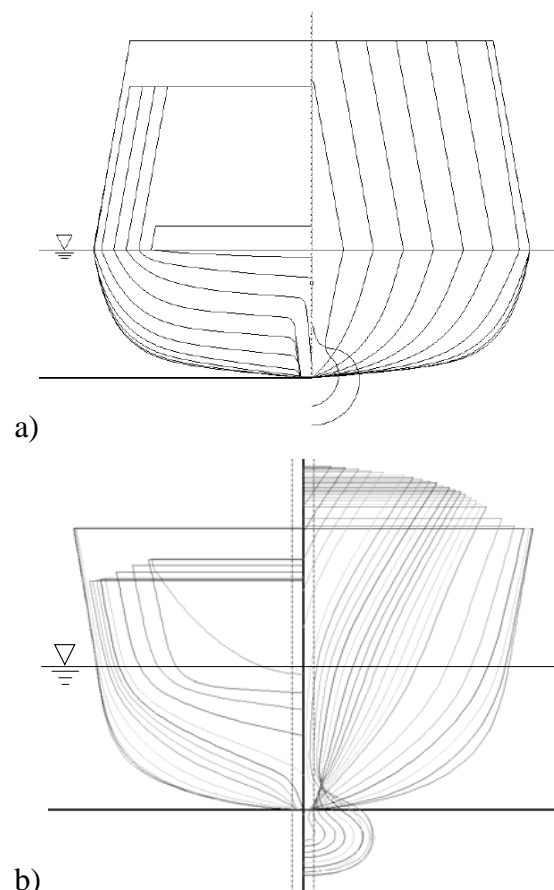


Figure 1. Body plans of hull forms used in the Force Study, a) ONRTH hull form b) Model 5514.

Table 1. Full-scale particulars of the ONRTH and Model 5514 hull forms

	ONRTH	Model 5514
Length (m)	154	142
Beam (m)	18.8	18.84
Draft (m)	5.5	6.51
Volume (m ³)	8540	9150
LCB (m aft of FP)	79.6	72.1
KG (m)	5.5	6.51
GM (m)	4.25	3.02

Simulated Conditions. As several of the computational tools employed in the numerical experiment do not incorporate full motion solvers, the investigation was designed to employ only prescribed motions, during which the forces and moments on a ship's hull were predicted throughout the motion cycle. The forces and moments were computed in a ship-fixed coordinate system with the origin at the center of gravity, with x positive toward the bow, y positive to port, and z positive upward. The moments were computed about the center of gravity.

The numerical experiment was divided into three tasks, each of which corresponds to one of the classical linear force decompositions, although at nonlinear amplitudes. Task 1 corresponded to the classic radiation problem, where the hull was forced to oscillate in calm water. Task 2 corresponded to the classic wave exciting force problem, where the hull was held fixed while it encountered waves. Task 3 was simulated motion in waves, where the vessel underwent prescribed motions in waves.

For Task 1, the hulls were forced in heave, pitch, and roll, while at zero speed and at a Froude number (F_N) of 0.3. For each of these modes of motion, the hulls were oscillated at frequencies of 0.2070 rad/sec, 0.3831 rad/sec, and 1.1 rad/sec. The hulls undergoing heave were forced at five amplitudes, varying from 5 to 80 percent of the calm water draft. For pitch, the hulls were forced at 5 pitch angles, varying

from 1° to 5°. Finally, roll was forced at five amplitudes, varying from 5° to 65°. The pitch and roll rotations were all prescribed about the center of gravity. In all modes, the maximum values were chosen to be well outside of the traditional linear regime, and well into the region where geometric nonlinearities could be expected to be significant.

Task 2 required simulation of the flow about the hulls, fixed at the calm waterline, in monochromatic waves of a single wave length; equal to the ship length ($\lambda/L = 1$). The calculations were performed at five equally spaced headings, from head to following seas, and at four wave steepnesses: $H/\lambda = 1/60, 1/20, 1/15, 1/10$. The flow was simulated at both zero speed and at $F_N = 0.3$. Again, the extreme wave steepnesses were selected to push the calculations into the region where the geometric nonlinearities would be significant.

Task 3 simulated large-amplitude motions in beam and following seas. In both conditions, the vessel was forced to move such that the heave amplitude equaled the wave amplitude, and at the center of gravity, the vessel's waterplane was tangent to the wave's surface. In the following-seas' condition, the vessel simulates heave and pitch motion; while in the beam-seas' condition, the vessel simulates heave and roll. For the following-seas' case, the wave length was chosen as twice the vessel length, $\lambda/L = 2$, and the wave steepness was chosen as $H/\lambda = 1/20$. The maximum pitch corresponded to the maximum wave slope and the pitch frequency was equal to the frequency of encounter. In the beam-seas' condition, the wave length was chosen as equal to the vessel length, $\lambda/L = 1$, and wave steepness was chosen as $H/\lambda = 1/10$. The maximum roll corresponded to the maximum wave slope, and the roll frequency corresponded to the wave frequency. In both cases, the amplitude of the vessel's motions was large, but the motions relative to the wave were small.

Simulation Tools Exercised. Eight simulation tools were chosen for use in the



Force Study. These are listed in Table 2, which provides the names of the codes, the abbreviations used to denote them on the plots of the results, a brief characterization of the theory incorporated in each code, and a bibliographic reference to each code. The codes were selected to provide a range of state-of-the-art capabilities. With the exception of FREDYN, all of the codes were run by their developers; FREDYN was run at NSWCCD.

The codes were selected to include fully linear theory, blended codes — as defined earlier in the paper, and nonlinear codes — although the extent of the nonlinearity varied. Most of the codes were three-dimensional codes, although two of them were strip theory codes: one linear (FREDYN) and one nonlinear (NSHIPMO).

Results. The size limitation on this paper precludes the presentation of all but a few of the results from the Force Study, which constitutes literally many 1000's of plots.

Table 2. Simulation tools included in the Force Study (2-D — strip theory, 3-D — fully 3-dimensional, L — linear theory, B — blended theory, NL — nonlinear theory).

Program Name	Abbreviation	Type of Theory	References
AEGIR-1	A1	3-D, L	Kring, et al. (2004)
AEGIR-2	A2	3-D, B	
FREDYN	FD	2-D, B	De Kat & Paulling (1989), de Kat 1994), de Kat, et al. (1994)
LAMP-1	L1	3-D, L	Liut, et al. (2002)
LAMP-3	L3	3-D, B	
LAMP-4	L4	3-D, NL	
NFA ¹	NF	3-D, NL	Dommermuth, et al (2006), Dommermuth, et

¹ Due to the fact that NFA required large amounts of computer time, it did not predict all of the cases discussed. Additionally, because the predicted forces were not decomposed into components, none of its results appear in the figures presented.

			al. (2007)
NSHIPMO	NS	2-D, NL	Telste & Belknap (2008) ²

From Task 1, time-histories of the vertical component of the radiation force on the ONRTH model during forced pitch of at $F_N = 0$ and $\omega = 1.1$ rad/sec is presented in Figures 2 and 3, for pitch amplitudes of 1° and 5°, respectively.

In Figure 2, the force time-histories for all of the computational tools, except LAMP-4 (L4) and NSHIPMO (NS), the two nonlinear codes, appear as similar sinusoidal curves.

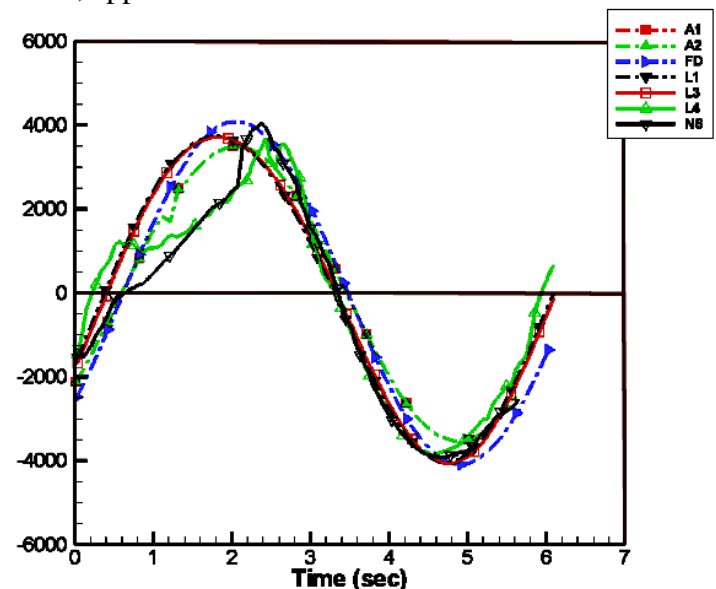


Figure 2. Time-history of ship-fixed vertical force from Task 1 predictions for ONRTH hull undergoing forced pitch at $F_N = 0$ and $\omega = 1.1$ rad/sec with a pitch amplitude of 1°.

² NSHIPMO has not been documented or reported. The description in Telste & Belknap (2008), based on a private communication from Prof. Robert F. Beck of the University of Michigan, provides the best description available.

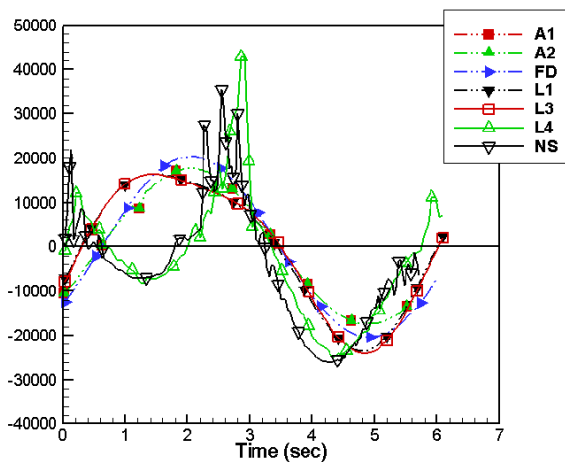


Figure 3. Time-history of ship-fixed vertical force from Task 1 predictions for ONRTH hull undergoing forced pitch at $F_N = 0$ and $\omega = 1.1$ rad/sec with a pitch amplitude of 5° .

This shows that all of the linear and blended codes, which have linear radiation forces, are producing quite similar results. For pitch amplitudes as small as 1° , the two nonlinear codes, LAMP-4 and NSHIPMO, show significant deviations from the linear radiation forces over a significant fraction of a cycle. The deviations from linearity are even more dramatic at 5° amplitude, where there is a significant deviation from the linear radiation force over the entire cycle. It is quite remarkable how similar the predictions are from the two nonlinear codes, considering that one is a strip theory and the other a 3-dimensional code. The noise in the predictions by the two nonlinear codes may be related to discontinuous jumps in geometry from one time step to another.

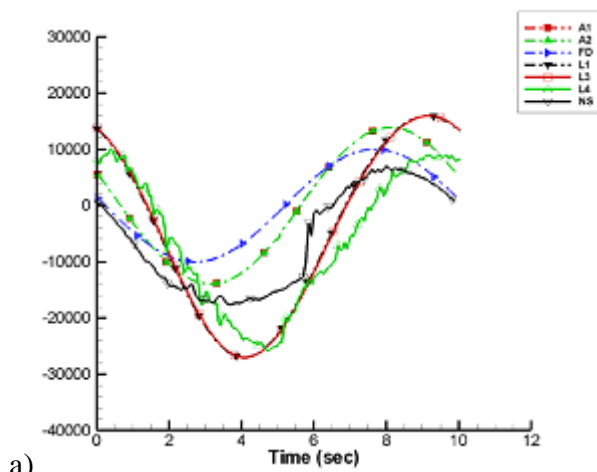
Figure 4 presents the vertical-force time history for a zero speed following-seas' case of the ONRTH hull in Task 2. The hull is at $F_N = 0$, and the wave length corresponds to $\lambda/L = 1$, with a steepness $H/\lambda = 1/15$. The force has been decomposed into three components: the diffraction force, the Froude-Krylov force, and the hydrostatic force.

There is more variation, compared to Task 1, amongst the force predicted by the

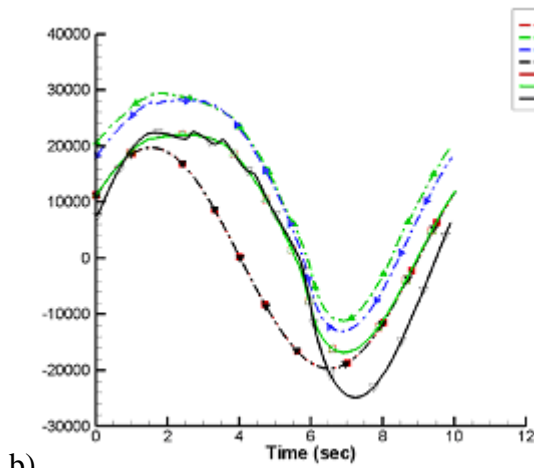
various codes for this case. This is in part due to known inconsistencies between how the various codes represent the incident waves and how the pressures on the hull are calculated. For instance, it is known that NSHIPMO uses Wheeler stretching (Wheeler, 1969) to correct the pressure within an incident wave to produce zero pressure on the incident wave surface. The LAMP codes use the fully nonlinear Bernoulli equation to compute the pressure for a linear wave. Some indications of the impact of this inconsistency for the incident wave appear in Figure 3.

The hydrostatic force calculations by the two linear codes present constant values, as anticipated, and are in agreement. The hydrostatic forces predicted by the blended and nonlinear codes are consistent with the exception of NSHIPMO, which varies, probably due to the use of Wheeler stretching.

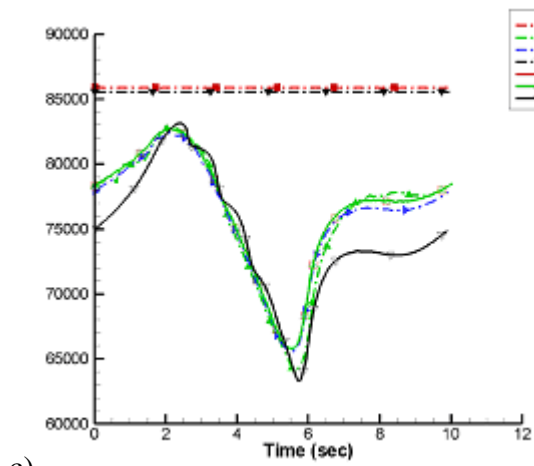
Task 3 predictions of the vertical force time-history from a following-seas' case for Model 5514 are presented in Figure 5. The hull is at



a)

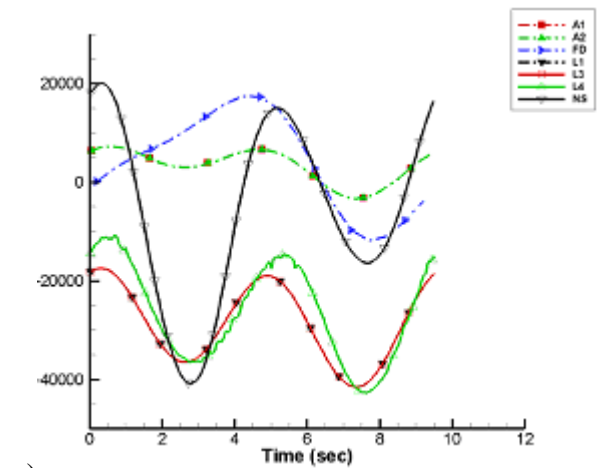


b)

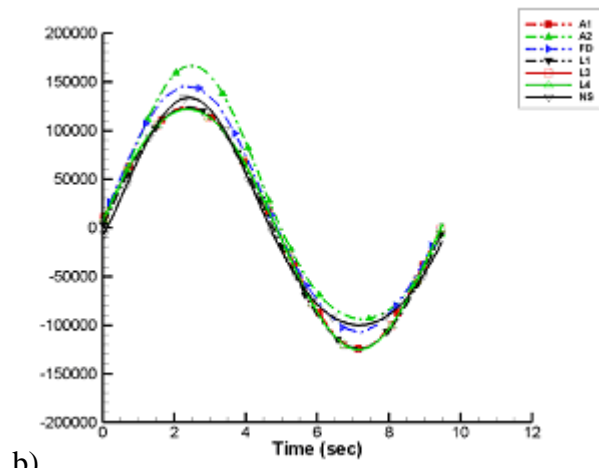


c)

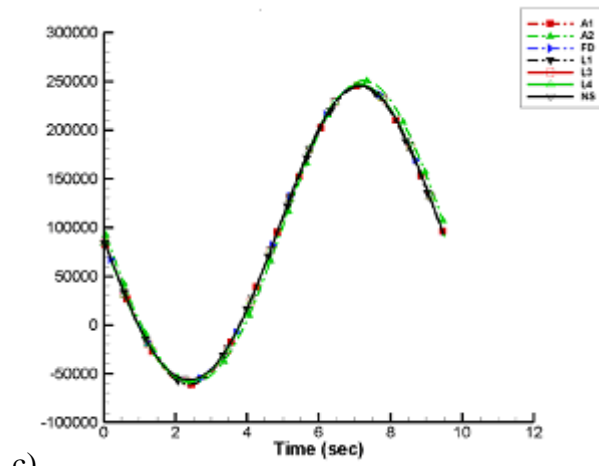
Figure 4. Time-history of the ship-fixed vertical force from Task 2 predictions for the ONRTH hull. The hull is at $F_N = 0$, in steep following seas, $\lambda/L = 1$, $H/\lambda = 1/15$, a) diffraction force, b) Froude-Krylov force, c) hydrostatic force. (Belknap & Telste, 2008).



a)



b)



c)

Figure 5. Time-history of ship-fixed vertical force from Task 3 predictions for Model 5514 hull, while contouring following seas at $F_N = 0$, $\lambda/L = 2$, $H/\lambda = 1/20$, a) hydrodynamic force, b) Froude-Krylov force, c) hydrostatic force. (Belknap & Telste, 2008).

$F_N = 0$, and the wave length corresponds to $\lambda/L = 2$, with a steepness $H/\lambda = 1/20$. As presented, the force has been decomposed into three components: the hydrodynamic (radiation and diffraction) force, the Froude-Krylov force, and the hydrostatic force.

The hydrostatic and Froude-Krylov forces shown in Figure 5 are an order of magnitude greater than the hydrodynamic forces. However, the hydrostatic and Froude-Krylov forces are 180° degrees out of phase with each other, so they largely cancel each other. Thus the difference between the hydrostatic and Froude-Krylov forces is the same order of magnitude as the hydrodynamic force, rendering an accurate calculation of the hydrodynamic force very important. Both the hydrostatic and Froude-Krylov forces calculated by all of the codes are in remarkable agreement — there is no difference in the hydrostatic force, and the differences in the Froude-Krylov force predictions are small. The hydrodynamic forces presented in Figure 5 show significant variation between the codes. As it was impossible to distinguish between the radiation and diffraction components of the hydrodynamic force, one cannot identify the sources of the difference. The AEGIR codes and FREDYN produced similar force levels, as did all of the LAMP codes, NSHIPMO predicted forces that vary between the AEGIR/FREDYN force levels and the LAMP force levels. It is not obvious why the three LAMP codes produced such similar forces. Although LAMP-1 and LAMP-3 produced the same force, as they should, this difference may be due to their use of the fully nonlinear form of Bernoulli's equation.

Conclusions from the Force Study. Thousands of calculations were made and compared of the forces and moments on two hulls: oscillating in various modes of motion in calm water, fixed in waves, and contouring waves. The results are presented in the form of time-history plots showing simulated ship motions at two speeds, for a variety of headings and wave/motion amplitudes. (These

results have also been compiled into a report containing 15,240 pages.)

It was not the purpose of the study to evaluate any one code relative to another, but rather to evaluate the differences between various complexities of theory. In general, codes with a consistent level of theory produced quite consistent results.

In many of the forces and moment predictions, the results from Task 1 demonstrated the importance of nonlinearity in the radiation forces. An obvious indicator of nonlinearity is the departure of the components of force and moment from a simple sinusoidal form. Spikes in the forces and moments may originate from the consideration of geometric nonlinearities.

The results from the Task 2 predictions indicated that a nonlinear wave model, as well as an appropriate evaluation of the pressure on the hull, is required. This subject area needs further investigation.

Task 3 showed that cancellation of forces and moments arising from the Froude-Krylov forces and hydrostatics indicated the importance of determining the wave radiation and diffraction force and moment components accurately, even when they are small.

A surprising finding was that the body-exact strip theory is capable of capturing important nonlinearities — comparable to the fully nonlinear 3-dimensional codes. This result provides hope for the development of fast codes to predict dynamic stability failures, on the order of real time.

2.2 Maneuvering in Waves

The state-of-the-art in the theory of maneuvering in waves is to superimpose a maneuvering model on a seakeeping code. Experience with several different maneuvering models has shown that a Abkowitz-type

maneuvering model (Abkowitz, 1969), which does an excellent job of predicting calm water maneuvering, produces nonsensical results in waves. To gain insight into this issue, an experiment was performed where the traditional maneuvering tests — turning circles and zig-zags, were run in both calm water and in regular waves, of varying wave lengths and steepnesses using a model of a combatant-type hull form.

Figures 6, 7 and 8 show the time-histories of a series of turning circles performed under identical conditions except for increased wave steepness. In each figure, the model was at $F_N = 0.3$, the rudder angle, δ , is 20° , and the wave length to model length, λ/L , was 1. Between the three figures, the wave steepness, H/λ , increased from $1/90$ to $1/60$ to $1/30$, respectively. Each figure shows the corresponding calm water turning circle as a dashed line and the turning circle in waves as a solid line. Each run was composed of 4-1/2 complete circles.

In Figure 6, for $H/\lambda = 1/90$, there was virtually no difference between the turning circles in calm water and in waves — the diameter is unchanged and there is no “drift” of the turning circle. The turning circles in waves in Figure 7, for $H/\lambda = 1/60$, shows no increase in the turning diameter, but there is a slight amount of drift in the turning circle, roughly 10 percent of the diameter over four and a half circles. The plot shows quite different results for the $H/\lambda = 1/30$ case, Figure 8. In this case, there is an increase in the turning diameter of about 10 percent, with significant drift of the circles — roughly 50 percent of the turning diameter over 4-1/2 turns. In shorter waves, the increase in turning diameter and drift occur in less steep waves than was examined for this case.

Although there is no consensus as to the source of this drift and the increase in turning diameter, one plausible explanation is the second-order drift force, which increases as the square of the wave amplitude. Although it is

also likely that there are other issues involving the interaction of maneuvering with ship motions in waves.

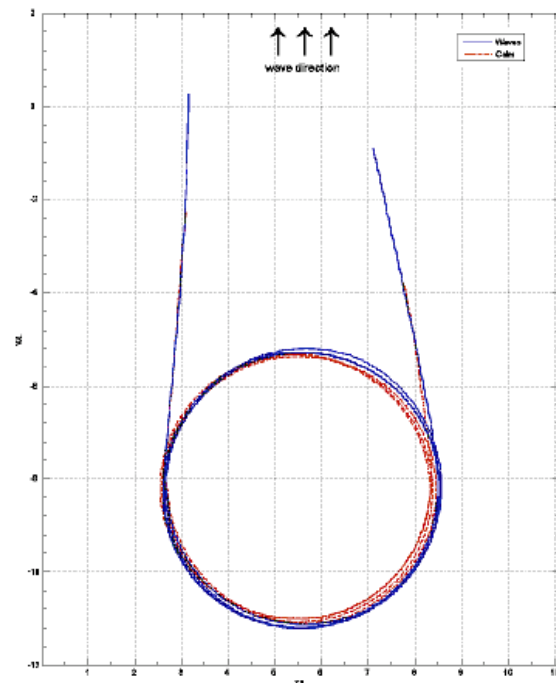


Figure 6. Time-history turning circle in waves, $F_N = 0.3$, $\delta = 20^\circ$, $\lambda/L = 1$, $H/\lambda = 1/90$; red dashed line in calm water, solid blue line in waves.

2.3 Large-amplitude Roll Damping

The state-of-the-art for predicting frequency-domain roll damping is the component-based model of Ikeda (Ikeda, et al., 1978; Himeno, 1981). This model is semi-empirical, and is based on small amplitude experiments with models of merchant hull forms. Time-domain roll damping is generally based on the Ikeda frequency-domain model, and uses averaging of the frequency-domain roll-damping components to produce the time-domain roll damping used in simulations. Thus, there is a need to develop a physics-based, time-domain roll-damping model, which is applicable to large-amplitude motions and naval vessels, as well as to commercial vessels.

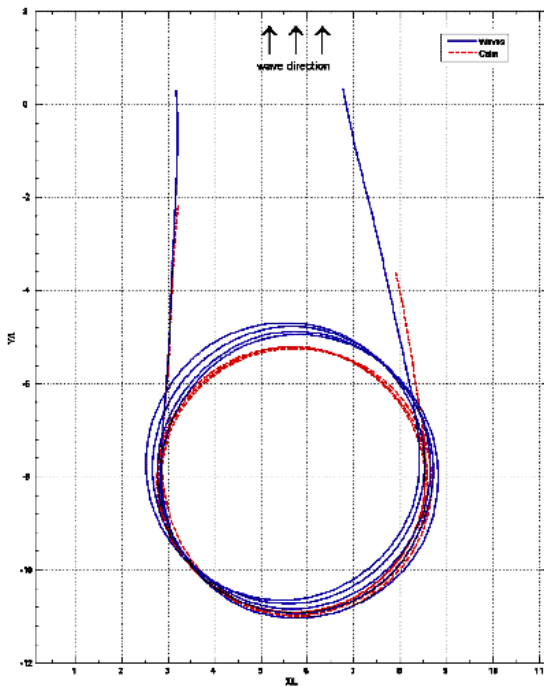


Figure 7. Time-history turning circle in waves, $F_N = 0.3$, $\delta = 20^\circ$, $\lambda/L = 1$, $H/\lambda = 1/60$; red dashed line in calm water, solid blue line in waves.

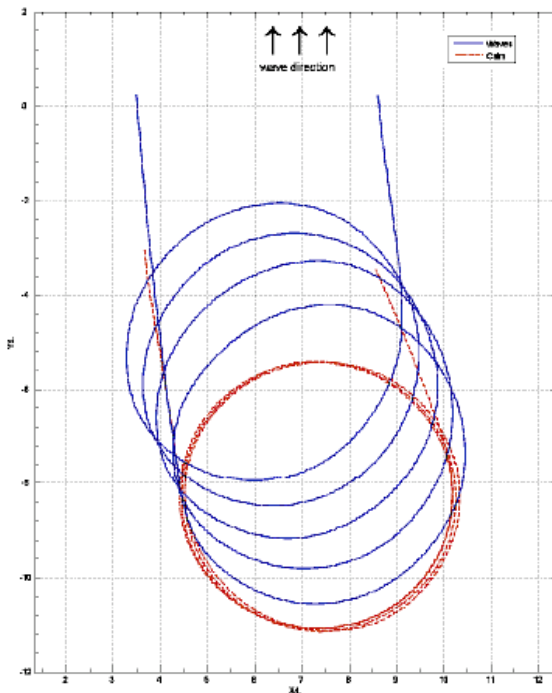


Figure 8. Time-history turning circle in waves, $F_N = 0.3$, $\delta = 20^\circ$, $\lambda/L = 1$, $H/\lambda = 1/30$; red dashed line in calm water, solid blue line in waves.

As discussed in Himeno (1981), frequency-domain roll damping is typically divided into seven components attributed to the hull, bilge keels, and rudder. Four of the components: friction, eddy making, lift, and wave making are attributed to the hull; and normal force, hull pressure, and wave-making roll damping are attributed to the bilge keels and rudder.

The seven terms are generally treated as linear, in the sense that in the equation of motion for roll, the roll-damping contribution to the equation of motion is only a linear function of the roll velocity. However, the coefficients multiplying the roll velocity may be functions of the roll frequency and the amplitude of the roll. In the frequency domain, this necessitates iteration for the values of roll damping, which correspond to the resulting amplitude of roll at each frequency.

This type formulation is not amenable for use in the time domain, except when reduced to some average representation, such as an equivalent linear damping. This may be adequate for small-amplitude roll, but it is not adequate when the amplitude becomes large. For instance, for many ships, when the roll angle reaches an angle of around 30° , one of the bilge keels emerges (Figure 9) and the bilge-keel roll damping is approximately halved — ignoring the potentially large transient associated with the bilge keel exiting and entering the water. Bilge-keel component predictions are also dependent on ship geometry, including bilge keel size, as well as roll amplitude. Although neglected, consideration of the bilge-keel wave-making damping and added mass effects at large roll should also be included (Bassler & Reed, 2009).

Modifications as elementary as adding a simple jump in the linear roll-damping coefficient at the angle for which the bilge keels emerge renders the total solution for the simple roll equation highly nonlinear, even in the frequency domain.

The US Navy has performed forced oscillation experiments (Bassler, et al., 2007; Fullerton, et al., 2008) to study these phenomena and determine roll-damping characteristics at large roll angles. Roll decay experiments have also been carried out with instrumented appendages — including bilge keels, rudders, and skegs, to assess their contribution to roll damping (Grant, et al., 2007; Etebari, et al., 2008). Initial comparisons between experimental results and unsteady RANS simulations have shown some promising results (Miller, et al., 2008).

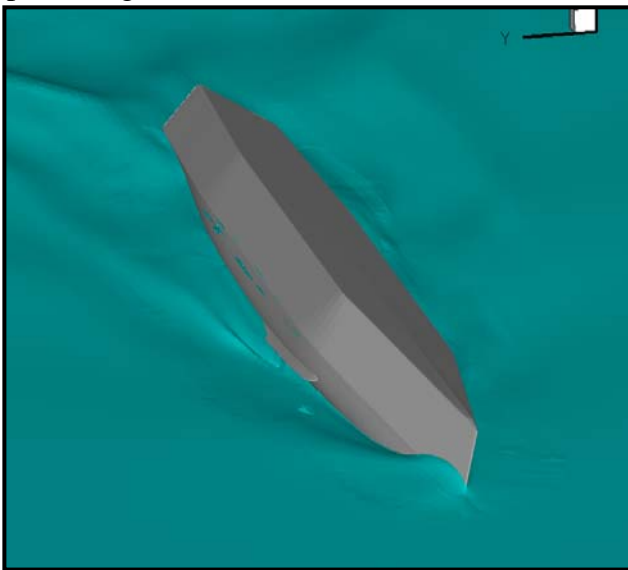


Figure 9. RANS simulation of the ONRTH, $F_N = 0.30$, $\omega = 4.83$ rad/s, $\phi = 30$ deg, where the bilge keel partially emerged from the water (Miller, et al., 2008).

In the time domain, it has been suggested that treating the ship with its bilge keels as a slender fish-like body (Lighthill, 1960; Newman & Wu, 1974; Newman, 1975) might provide a reasonable analytical basis. Another path the US Navy is currently exploring is the application of low-aspect lifting-surface theory, as studied by Bollay (1936, 1939), Gersten (1961, 1964), and van Zwol (2004) for steady flows, and by Brown & Michael (1954, 1955) and Howe (1996) for unsteady vortex shedding.

3. VERIFICATION, VALIDATION AND ACCREDITATION³

If decisions regarding the design and construction of ships, each costing hundreds of millions of dollars, if not a few billion dollars, are going to be made based on the stability predictions of a simulation tool, there must be a reasonable assurance that the tool provides acceptably accurate results. The process by which a tool may be determined to be sufficiently accurate is known as verification, validation and accreditation (VV&A).

3.1 An Overview of VV&A

The definition of VV&A follows. Quoting from a US Navy VV&A presentation, “Verification, Validation, and Accreditation are three interrelated but distinct processes that gather and evaluate evidence to determine, based on the simulation’s intended use, the simulation’s capabilities, limitations, and performance relative to the real-world objects it simulates.” Beck, et al. (1996); AIAA (1998); and DoD (1998, 2003, 2007) provide different, although consistent, definitions of the three components of VV&A. The DoD definitions for these three terms are provided below, each followed by a practical commentary relevant to computational tools for predicting dynamic stability.

Verification — the process of determining that a model or simulation implementation accurately represents the developer’s conceptual description and specification, i.e., does the code accurately implement the theory that is proposed to model the problem at hand?

Validation — the process of determining the degree to which a model or simulation is an accurate representation of the real world from the perspective of the intended uses of the model or simulation, i.e., does the theory and the code that implements the theory accurately

³ An expansion of Reed (2008)

model the relevant physical problem of interest?

Accreditation — the official determination that a model or simulation, . . . is acceptable for use for a specific purpose, i.e., is the theory and the code that implements it adequate for modeling the physics relevant to a specific platform? In other words, are the theory and code relevant to the type of vessel for which it is being accredited?

US Navy experience with attempting to verify ship-dynamics' software has been that the documentation for many hydrodynamic codes, particularly the theoretical basis, is neither complete nor rigorous enough for the verification process to be separated from the validation process. Under these circumstances, when one finds that the computations do not adequately model the physical reality, one is left to ponder whether the code is not accurately modeling the intended physics or whether the intended physics are not adequate for the problem. In this case, the dilemma becomes: should one attempt to debug the code or should one abandon use of the code because its underlying physics model is not adequate? Attempting to resolve this dilemma can be expensive, in terms of both time and money.

Another issue related to verification of software is the actual quality of the code and the documentation of the code itself. Often the coding does not follow any consistent standard and there is often insufficient guidance to link the actual code back to its theoretical basis.

As for the actual verification of the code, this is best done by means of unit tests, where each module and block of modules is exercised against known or expected solutions. When properly constructed, these unit tests will not only test the module against normal execution, but also against unexpected or unanticipated inputs, to determine if the code handles error exceptions correctly via error traps or error returns. Many codes are not designed robustly enough so as to deal with anomalous inputs—

they expect that the input will always be correct and that all modules that produce input for other modules provide correct input. Rationally, this is a rather naïve assumption.

A second observation with regard to VV&A relates to the question of how one performs validation for a code used for predicting total (as opposed to partial) dynamic stability failures, events that are essentially binary. Either there was a failure or there was not. One can certainly contemplate comparing the failure predictions from a simulation to a model test or full-scale vessel. However, the failure is hopefully a rare occurrence and is fraught with many unknowns: What were the actual local environmental characteristics at the instant of failure and in the few minutes leading up to failure?; What were the actual mass properties of the vessel at the time of failure?; Was the vessel actually intact at the time of failure, or had it in fact taken on water, leading to a failure in what was actually a damaged state?; Was the vessel on autopilot or under manual steering, etc.? In the case of model-scale tests, some of the full-scale issues can be resolved, but for a free-running model it is still difficult to characterize the waves that the model is encountering, particularly if they are irregular seas. The question of the autopilot steering algorithms is particularly challenging: Can a simulation accurately model the actions of a helmsman?; What is the range of human performance or the actual autopilot on the vessel?; Particularly in these days of smart autopilots that “learn,” can the actual autopilot algorithm in the time leading up to the instant of failure be known? Thus, there are a number of issues that must be resolved before one can conclude that any computational tool is ready to use for establishing performance-based stability criteria, or certifying a ship design as meeting the criteria.

In order to accommodate the validation of simulations for predicting stability failures, situations must be examined that are not easily characterized using techniques that are routinely used for seakeeping validation.

Nonlinear dynamics methods appear to show significant promise. There are two aspects of nonlinear dynamics that appear to apply to validation. The first is nonlinear time-series analysis and the second is bifurcation analysis.

3.2 Nonlinear Time-Series Analysis

In nonlinear time-series analysis (cf. Kantz & Schreiber, 2004), the same time-series analysis is applied to motions measured on a physical model (or ship) and to simulations of the same vessel, in the same environment, as observed during the measurements. The results of the two sets of analysis are compared to each other, often graphically, to determine whether they have produced similar results.

McCue, et al. (2008) provide examples of nonlinear time-series analysis, applied as it might be for validation of simulations. Both qualitative and quantitative metrics that may apply were examined. Some qualitative measures include: reconstructed attractors, correlation integrals, recurrence plots, and Poincaré sampling; possible quantitative measures are: correlation dimension, Lyapunov exponent comparison, system entropy, and approximations to the equations of motion (EOM).

Figure 10 presents two figures from McCue, et al. (2008) that compare recurrence analysis of measured data from DTMB Model 5514 (Hayden et al., 2006) to numerical simulations. The recurrence plot presents graphically how often a motion trajectory in state space returns to a trajectory near the initial one. State variables include quantities such as roll angle, roll velocity, pitch angle, and pitch angular velocity. In generating a recurrence plot, all quantities are nondimensionalized by their standard deviation. The quantity ε is the distance allowance between the two states, so the smaller ε is, the closer two states must be to correlate. As can be observed, there is a significant difference in the density of points

between these two recurrence plots for the same conditions. Figure 11 provides the correlation integral, which represents the density of the data on the recurrence plot versus ε , for both the measured model data and the numerical simulations. As is seen, there is a significant difference in the slopes between the two figures, indicating that the simulation is missing some aspect of the experimental results

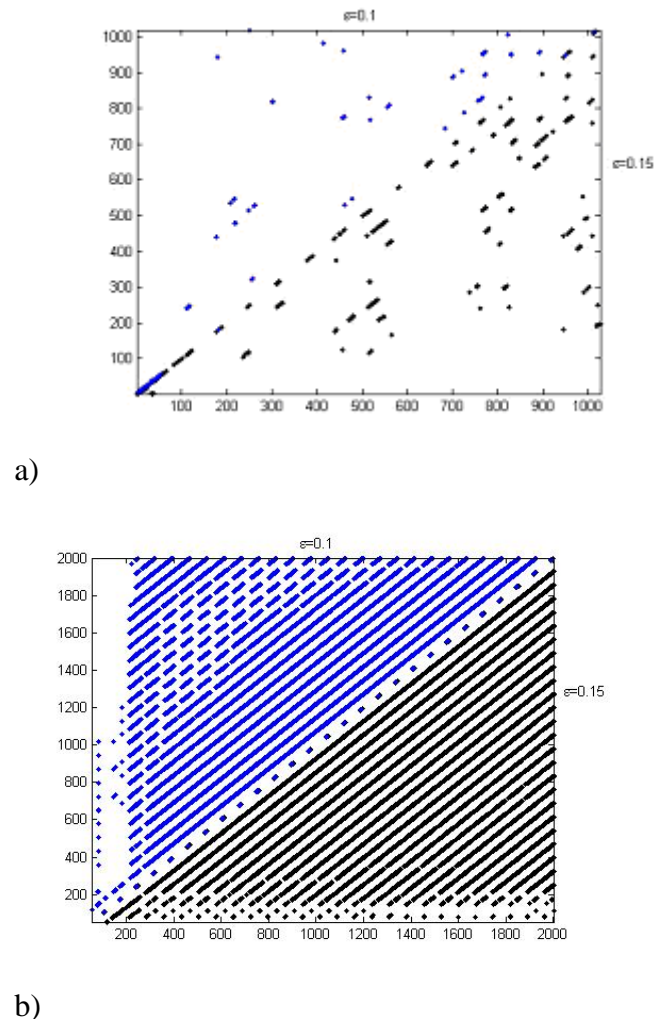
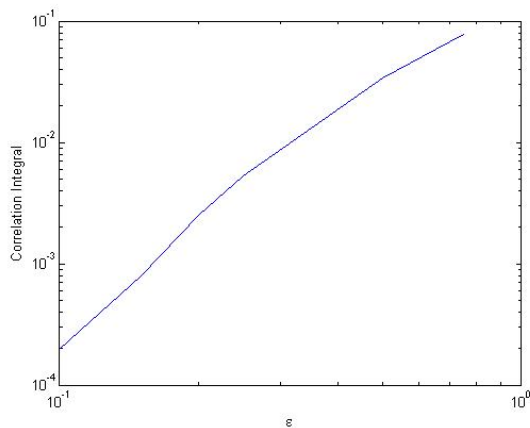


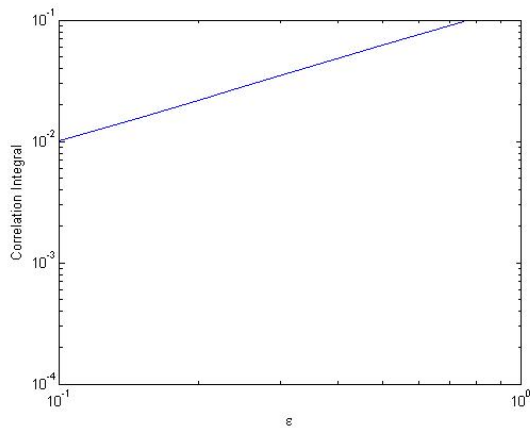
Figure 10. Recurrence plot for DTMB Model 5514 Run 312, $\varepsilon = 0.15$ below the diagonal, $\varepsilon = 0.1$ above the diagonal, a) measured data, b) numerical simulation. (McCue, et al., 2008).

Figure 12 shows phase space and Poincaré plots for the same run from Hayden, et al. (2006), as described for Figures 10 and 11. The phase plot is the standard plot in which displacement is plotted against velocity, in this case roll angle against roll-angular velocity. The Poincaré component of the plot, the plus

signs, shows the displacement and velocity at a common time interval, in this case 36.5 seconds, full scale. If the motions are purely periodic, then the points will converge, as in Figure 5b, while if the motion is not periodic at the selected period, they will not converge to a single location. This figure shows quite different shapes for the trajectories in phase space, and the Poincaré sampling shows convergence for the computed results and quite scattered results for the model experiments.



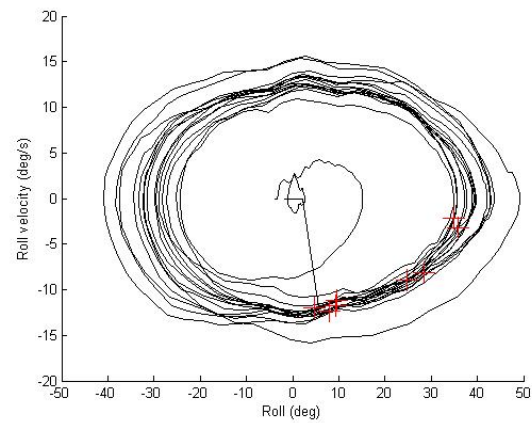
a)



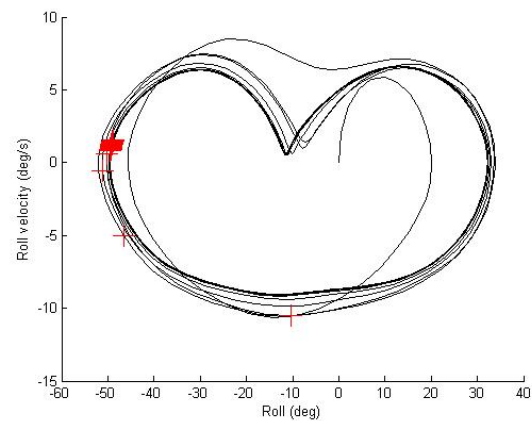
b)

Figure 11. Correlation integral versus ε for DTMB Model 5514 Run 312, a) measured data, b) numerical simulation. (McCue, et al., 2008).

While nonlinear time-series analysis techniques can easily illustrate differences between measurements and predictions, there is still much to be investigated. The range of time-series analysis techniques which may be applicable to dynamic-stability failure prediction certainly has not been exhausted. However, these comparisons are at best qualitative; quantitative methods, particularly for physical understanding and for comparing experimental and computed results, are needed. Bifurcation analysis techniques may provide this necessary additional insight.



a)



b)

Figure 12. Phase space and Poincaré plot for DTMB Model 5514 Run 312 with Poincaré sampling every 36.5 seconds., a) measured data, b) numerical simulation. (McCue, et al., 2008).



3.3 Bifurcation Analysis

There are at least four bifurcations that have been observed in ship dynamics which could be used to analyze whether or not a dynamic-stability code is producing the correct dynamic behavior: Fold bifurcation, Flip bifurcation, Hopf bifurcation, and Homoclinic bifurcation. All of these bifurcations are discussed in Belenky & Sevastianov (2007). Bifurcation analysis would appear to be appropriate for application to the lateral-plane aspects of dynamic stability. A brief discussion of these bifurcations follows.

Fold bifurcation (also known as tangent instability, jump to large-amplitude, or hysteresis) can be found in roll and yaw (Spyrpou, 1997; Belenky & Sevastianov, 2007: Sect. 4.5.2 for roll, Sect. 6.5.6 for yaw). It is responsible for direct broaching, and is observed as a dramatic increase in the response amplitude, with a small change of control parameter — usually excitation frequency for roll and commanded heading for yaw. Fold bifurcation can be detected when the eigenvalues of the variation equation are real and leave the unit circle in a positive direction. It has been observed in a model test reported by Francescutto, et al. (1994).

Flip bifurcation, which is also known as period doubling instability, can be found in roll and yaw (Spyrpou, 1997; Belenky & Sevastianov, 2007: Sect. 4.5.3 for roll, Sect. 6.5.6 for yaw). It is observed first as a loss of symmetry of a phase trajectory (the cycle becomes egg shaped), followed by a series of period doublings, eventually leading to deterministic chaos. Flip bifurcation can be observed when the eigenvalues are real and leave the unit circle in a negative direction. A chaotic stage of the bifurcation can be detected when the Melnikov function crosses zero. In this case, branches of the invariant manifold have an infinite number of intersections, resulting in fractalization of the safe basin.

Hopf bifurcation, also known as flutter, can be found for surge in stern-quartering seas (Spyrpou, 1996; Belenky & Sevastianov, 2007: Sect. 6.5.2). Hopf bifurcation can be observed as relatively small-amplitude oscillations around the surf-riding equilibrium. It can be detected by a combination of the limit cycle with unstable focus equilibrium. It has been observed in a model test by Kan (1990).

Homoclinic bifurcation can be found in surge (Belenky & Sevastianov, 2007: Sect. 6.3.5), and is responsible for surf-riding. It is observed as the appearance of an equilibrium co-existing with periodical surging, then as the only option. The control parameter for this bifurcation is the nominal Froude number. Homoclinic bifurcation can be detected in the phase plane as the connection of a saddle point to itself (or to a saddle point on the next wave). It is reported as having been observed in both full-scale and numerous model tests.

Bifurcation analysis has not been formally reported as a code validation technique, but in conjunction with analytical models of dynamic instabilities and model- and full-scale observations, appears to show promise as a validation technique — does the code demonstrate the physical bifurcation behavior that would be expected, based on analytical models and experimental observations?

Spyrou, et al. (2009) employed continuation analysis, in conjunction with a specialized version of LAMP (Liut, et al., 2002), to examine the occurrence of surf-riding and broaching. Figure 13 provides an example of the results that they have produced.

While the work of Spyrou, et al. (2009) was not constructed as a validation study, what they have done indicates that some type of bifurcation analysis has promise as a validation technique. This is a line of investigation that should be pursued further.

3.4 The Problem of Rarity

Another issue for the VV&A of simulations for dynamic stability is the “problem of rarity,” where the time between events is long compared to the wave period (Belenky, et al., 2008a,b). Large numbers of realizations may be required to observe dynamic stability failures, either in a simulation or experimentally.

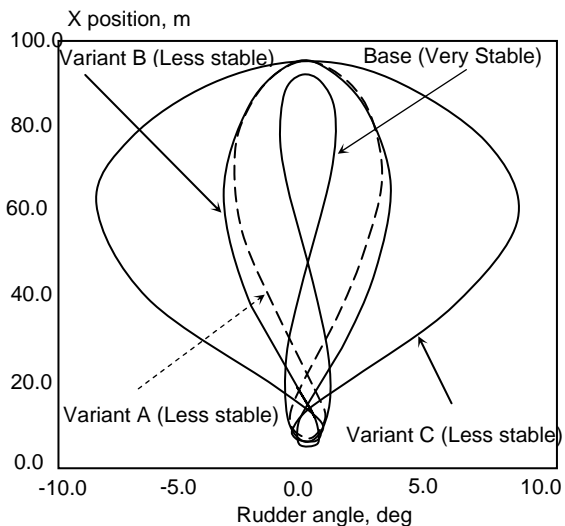
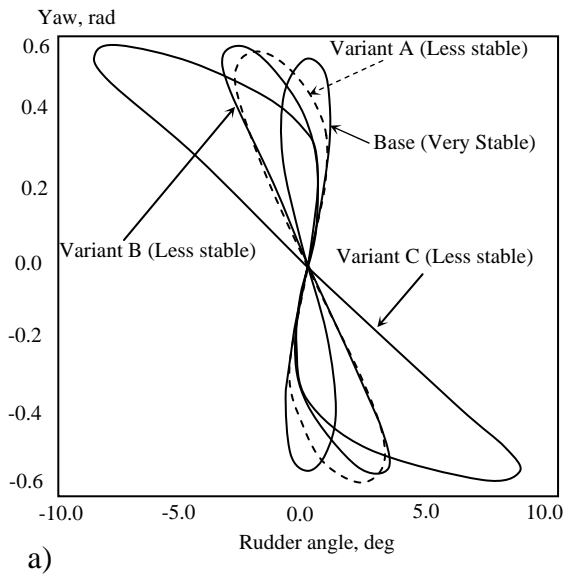


Figure 13. Output of LAMPCont for the sample ship in quartering seas, illustrating some of the stability variants with a fixed propeller speed in a wave, $\lambda = 200$ m and $H = 4$ m, a) ship’s yaw angle relative to the wave direction vs. rudder deflection, b) position of the ship CG on the wave relative to the wave crest. (Spyrou, et al., 2009)

Even if these events are observed, direct comparison between realizations is difficult due to the stochastic nature of the failure event. One method that may help to resolve this problem is the use of deterministic critical-wave groups. This would enable direct comparison of realizations, while also capturing the worst-case conditions of the stochastic environment necessary to assess the ship’s stability performance. Themelis & Spyrou (2007, 2008) demonstrated the production of deterministic critical-wave groups using simulation tools, and Bassler, et al. (2009) has shown that it may also be possible to produce them experimentally.

4. PERFORMANCE-BASED CRITERIA⁴

With few exceptions, the navies of the world are still employing hydrostatic-based stability criteria, which reflect outgrowths or extensions of the works of Rahola (1939) and Sarchin & Goldberg (1962). However, the need to develop risk-based stability criteria is recognized.

There have been a number of recent papers and reports relating to the subject of dynamic stability assessment, cf. Alman, et al. (1999), McTaggart (2000), McTaggart & de Kat (2000), and Hughes (2006). Many of these have been motivated by the work of the Naval Stability Standards Working Group (NSSWG) a collaborative effort between the Royal Australian Navy, the Canadian Navy, the Royal Netherlands Navy, the British Royal Navy, the US Coast Guard, and the US Navy.

The following subsections summarize the current status of several naval stability standards: NATO, Naval Stability Standards Working Group (NSSWG), and the US Navy. The US Navy standard appears to be the first quantitative performance-based standard.

⁴ Based on the author’s section on naval standards in ITTC (2008).



4.1 Existing Naval Stability Standards

In 2003, NATO initiated an effort to develop a goal-based standard for naval vessels that could guide navies and classification societies in the development of rules for naval vessels. The intent was to develop regulations for naval vessels that paralleled the IMO regulations for commercial vessels (IMO regulations do not apply to naval vessels). In 2007, NATO issued several documents relating to standards for classing naval vessels, all under the umbrella of a Naval Ship Code (NATO, 2007a). The introduction to the Naval Ship Code states, "The overall aim of the Naval Ship Code is to provide a framework for a naval surface-ship safety-management system based on and benchmarked against IMO conventions and resolutions that embraces the majority of ships operated by Navies." The code further goes on to state "... it therefore contains safety-related issues that correspond in scope to that which is covered by IMO publications but which reflect the fundamental nature of naval ships." Rudgley, et al. (2005) provided an overview of the process and the overall philosophy for the development of the Naval Ship Code.

The Naval Ship Code is composed of ten chapters:

Chapter I	General provisions
Chapter II	Structure
Chapter III	Buoyancy and Stability
Chapter IV	Machinery Installations
Chapter V	Electrical Installations
Chapter VI	Fire Safety
Chapter VII	Escape, Evacuation and Rescue
Chapter VIII	Radiocommunications
Chapter IX	Safety of Navigation
Chapter X	Carriage of Dangerous Goods

Chapter III, Buoyancy and Stability, includes dynamic stability and capsize. This chapter was developed in the second half of 2006 by a study group composed primarily of representatives from: Australia, Canada, Italy, Netherlands, Spain and the United Kingdom, with input from the Naval Stability Standards

Working Group (NSSWG). In parallel to the Naval Ship Code, NATO produced another document, Guide to the Naval Ship Code (NATO 2007b). The discussion of Chapter III in the Guide states "Due to the variety of available Naval Standards on stability and on-going work in other bodies to understand the dynamics of the stability problem and the measure of safety provided by current standards, it was decided not to develop another detailed quasi-static stability standard." Thus, the Naval Ship Code provides only the most generic guidance with regard to dynamic stability and capsize.

The Buoyancy and Stability chapter is divided into eight "Regulations" numbered 0 through 7. Regulations 1–7 are subdivided into four sections: Functional Objectives, Performance Requirements, Verification Methods, and Definitions (optional). Four of these Regulations (0-Goal, 1-General, 4-Reserve of Stability, and 7-Provision of Operational Information), explicitly mention capsize or dynamic stability. The Regulation 0-Goal specifically states:

- 1 The buoyancy, freeboard, main subdivision compartment and stability characteristics of the ship shall be designed, constructed and maintained to:
- 2 Provide adequate stability to avoid capsizing in all foreseeable intact and damaged conditions, in the environment for which the ship is to operate, under the precepts of good seamanship.

The "Performance Requirements" listed under Regulation 1-General further elaborate:

- 4 The ship shall:
 - 1 Be capable of operating in the environment defined in the Concept of Operations Statement.
 - 2 Have a level of inherent seaworthiness including motions tolerable by equipment and persons onboard, controllability

and the ability to remain afloat and not capsize.”

- 3 Be designed to minimize the risk faced by hazards to naval shipping including but not limited to the impact of the environment causing dynamic capsize, broach or damage to crew & equipment”
- 4 Be provided with operator guidance, as required in Regulation 7- Operator Guidance, to facilitate safe handling of the ship.

The “Verification Methods” section of Regulation 1-General states:

- 6 Verification that the ship complies with this chapter shall be by the Naval Administration.
- 7 The burden of verification falls upon the Naval Administration. All decisions that affect compliance with the requirements of this chapter shall be recorded at all stages from Concept to Disposal and these records be maintained throughout the life of the ship.

Thus the *Naval Ship Code* contains no specific dynamic-stability or capsize criteria, nor does it specify any procedures by which a vessel can be determined to be in compliance with the Code. Neither Regulation 4-Reserve of Stability nor Regulation 7-Provision of Operational Information provides any additional detail on how the requirements are to be met.

4.2 Developments Relating to Standards for Navies

Among other topics, the NSSWG has been examining existing naval stability standards against a dynamic stability metric. Hughes (2008) presents preliminary results of this study. In the study, a wide variety of static stability metrics (16 in total) for 12 naval

vessels have been correlated against a dynamic stability assessment performed using an older version of FREDYN (De Kat & Paulling, 1989; de Kat, 1994; de Kat, et al., 1994). The correlation coefficients for many of these metrics (e.g. GM , GZ_{max} , GZ_{30° , ϕ_{range} , $A_{0^\circ-40^\circ}$, $A_{0^\circ-\phi_{range}}$, etc.) were all in the high 0.8s or 0.9s (the majority were in the 0.9s, many were in the 0.99s). There was no static-stability parameter or metric that consistently had the highest correlation coefficient across all 12 ships. This indicates that the current static stability-based naval stability standards are not significantly deficient—at least for ships that fit the current hull-form mold. However, it should be noted that there is no means to determine how much stability margin any of these ships have.

The NSSWG is continuing its assessment of existing naval stability standards. It is anticipated that the FREDYN correlation will be repeated with an updated version of the code. However, this will require substantial computational effort and will not be undertaken lightly.

4.3 US Navy Stability Criteria

The one navy that has been identified as applying a performance-based dynamic-stability criteria is the US Navy. Based on some model tests of tumble-home hull forms in the late 1990s, it was found that the criteria of DDS 079-1 (US Navy, 2003) did not provide the equivalent margin against capsize for tumble-home ship designs as it does for traditional wall-sided and flared designs. Therefore, an intensive effort was instituted in 2000 to develop a dynamic stability-based standard.

Current US Navy dynamic-stability criteria is a relative criteria, whereby the new vessel design is assessed against an existing naval vessel designed for an equivalent mission — this ensures that a frigate is not judged against an aircraft carrier, or vice versa. The dynamic-



stability criteria has five components, which are as follows:

- a. The annual probability of capsize without wind effects, for the appropriate range of sea states, when multiplied by a margin of 1.10, is less than or equal to that of the equivalent mission benchmark ship.
- b. For each sea state, the capsize probability shall be determined for the specified range of modal periods. The worst-case capsize probability for each sea state/modal period multiplied by a factor of 1.10 shall be less than or equal to that of the worst capsize risk for the benchmark ship taken in the same sea state over the same range of speeds, headings, and modal periods.
- c. In any given sea state, it is shown on the capsize- and broaching-risk polar diagrams, that regions of high capsize probability, 60 percent or higher, are not adjacent to regions of high broaching probability, 60 percent or higher.
- d. Regions of zero capsize probability, as shown on a capsize-risk polar diagram, do not transition to regions of 80 percent or higher capsize probability over a 5-knot range of speed or 15° heading change.
- e. There shall be no region of 100 percent capsize probability in the defined mission sea states.

These criteria are applied over a range of sea states and modal periods. The sea states range from 5 to 8, with sea states 7 and 8 being subdivided into three significant wave heights, each of which has three modal periods. For each significant wave height and modal period, an assessment of capsize probability is performed over a range of speeds, 0 to 30 kt in 5-kt increments, and headings, 0° to 180°, in 15° increments. For each speed-heading combination, twenty-five 30-minute simulations are performed in a different realization of the sea state being investigated, resulting in up to 12-1/2 hours of simulated operation at each speed-heading combination.

Component (a) of the US Navy dynamic-stability criteria is intended to determine that the overall capsize risk is acceptable. Component (b) ensures that the capsize risk in all of the sea states is not excessive, by limiting it to being no worse than the worst risk for the benchmark ship. Component (c) is intended to ensure that the ship has a region of the speed-polar plot where it can operate without having to choose between having a high risk of either a capsize or broach, while (d) ensures that there are no locations where the ship transitions too rapidly in speed or heading from safe operation to high risk of capsize, and finally, (e) ensures that there are no absolutely unsafe areas on the capsize-speed polar plot where the ship has a 100 percent probability of capsize.

The implementation of the above standard has four components. The first component defines the code to be used for the assessment and the physical model against which the code will be validated. The second component defines the process for setting up the computational-model simulation of a ship for the dynamic stability. The third component defines the code validation process against model tests, and the criteria for the validation process. Finally, the last component provides the details of the capsize-risk assessment.

The motivation for the US Navy to employ a relative capsize-risk assessment approach was the recognition that simulation tools are not absolutely accurate, but it was assumed that the biases of the code would be independent of the details of the hull form. There are two major weaknesses of the US Navy's relative capsize criteria. The first is that there is no way of knowing the level of safety or margin that the benchmark ship has against capsize. The second relates to the assumption that the computational tools will have a uniform bias against all hull forms — the reality is that it has been found not to be consistently true, although it is not clear why.

To supplement the relative capsize-risk assessment methodology just described,

Belknap, et al. (2005) investigated a methodology for assessing annual- and lifetime-capsize risk based solely on regular-wave capsize model tests. This methodology relies on mapping the model test-based capsize probabilities onto the joint-probability distribution of a given wave length and period in both a given sea state and in a modal period. This joint-probability distribution is based on the work of Longuet-Higgins (1957). The results of these calculations indicate that the lifetime capsize risk for a typical naval vessel is on the order of a fraction of a percent. Intuitively, this seems to be a reasonable absolute lifetime capsize risk. However, many issues relating to the linear superposition of nonlinear experimental results, using the decomposition of nonlinear seas by means of a joint-probability distribution, need to be resolved regarding this methodology.

5. CONCLUSIONS

From a naval perspective, three areas critical to the performance of vessels in extreme seas have been discussed: physics of large-amplitude motions; verification, validation and accreditation (VV&A) of tools for these conditions; and performance-based criteria.

Hydrodynamic forces, maneuvering in waves, and large-amplitude roll damping have been highlighted as being very important to the physics of large-amplitude motions. The Force Study that examined the impact of large-amplitude responses in calm water, large-wave amplitudes on wave excitation, and prescribed large-amplitude motions in beam and following seas on hull forces was introduced. For maneuvering in waves, the impact of waves of increasing amplitude on the traditional calm-water turning circles was described. Some concerns regarding the prediction of damping in the time domain for large-amplitude roll motions was also introduced.

In VV&A, the challenge is performing this function for extreme-seas' conditions where

linear concepts such as response-amplitude operators are not applicable. The use of nonlinear time-series analysis and bifurcation analysis in validation were discussed as possible techniques, and some example were provided.

Performance criteria have been discussed from a naval perspective. The current NATO criteria are presented, along with the current NSSWG efforts. The US Navy's dynamic-stability criteria are introduced.

6. ACKNOWLEDGMENTS

The author would like to thank Vadim Belenky for his discussions regarding the paper, particularly those relating to the bifurcation analysis; John Telste and Tim Smith for the data plots they provided; Chris Bassler for his production support and editorial comments; and Suzanne Reed for her editorial work on this paper.

7. REFERENCES

- Abkowitz, Martin A. (1969) Stability and Control of Marine Vehicles. MIT Press, Cambridge, MA, vi+352 p.
- AIAA (1998) "Guide for the Verification and Validation of Computational Fluid Dynamics Simulations." AIAA G-077-1998 Guide, American Institute of Aeronautics and Astronautics.
- Alman, P. R., P. V. Minnick, R. Sheinberg & W. L. Thomas, III (1999) "Dynamic capsize vulnerability: Reducing the hidden operational risk." Trans. SNAME, **107**:245–80, Jersey City, NJ.
- Bassler, C., J. Carneal, & P. Atsavapranee (2007) "Experimental Investigation of Hydrodynamic Coefficients of a Wave-Piercing Tumblehome Hull Form," Proc. 26th Int'l Conference on Offshore Mech-



- anics and Arctic Engineering, OMAE2007, San Diego, CA.
- Bassler, C. C. & A. M. Reed (2009) "An Analysis of the Bilge Keel Roll Damping Component Model." Proc. 10th Int'l Conf. Stability of Ships and Ocean Vehicles (STAB 09), St. Petersburg, Russia, 17 p.
- Bassler, C. C., M. J. Dipper, & G. E. Lang (2009) "Formulation of Large-Amplitude Wave Groups in an Experimental Model Basin." Proc. 10th Int'l Conf. Stability of Ships and Ocean Vehicles (STAB 09), St. Petersburg, Russia, 13 p.
- Beck, R. F. & A. M. Reed (2001) "Modern Computational Methods for Ships in a Seaway." Trans. SNAME, **109**:1–51, Jersey City, NJ.
- Beck, R. F., A. M. Reed & E. P. Rood (1996) "Application of modern numerical methods in marine hydrodynamics." Trans. SNAME, **104**:519–37, Jersey City, NJ.
- Belenky, V. L., J. O. de Kat & N. Umeda (2008a) "Toward Performance-Based Criteria for Intact Stability." Marine Tech., **45**(2):122–123.
- Belenky, V. L. & N. B. Sevastianov (2007) "Stability and safety of ship: Risk of Capsizing." Second Edition. SNAME, Jersey City, NJ, xx+435 p.
- Belenky, V., K. M. Weems, W-M. Lin (2008b) "Numerical Procedure for Evaluation of Capsizing Probability with Split Time Method" Proc. 27th Symp. Naval Hydro., Seoul, Korea, 25 p.
- Belknap, W. F., B. L. Campbell, M. J. Dipper & W. T. Lee (2005) "Method for Computing Relative Annual and Lifetime Capsize Risks," Carderock Division, Naval Surface Warfare Center Report NSWCCD-50-TR-2005/085, 26 p.
- Belknap W. & J. Telste (2008) "Identification of Leading Order Nonlinearities from Numerical Forced Motion Experiment Results." Proc. 27th Symp. Naval Hydro., Seoul, Korea, 18 p.
- Bishop, R. C., W. F. Belknap, C. Turner, B. Simon & J. H. Kim (2005) "Parametric Investigation on the Influence of GM, Roll Damping, and Above-Water Form on the Roll Response of Model 5613." Carderock Division, Naval Surface Warfare Center Report NSWCCD-50-TR-2005/027, 185 p.
- Bollay, W. (1936) "A New Theory for Wings with Small Aspect Ratio." Ph.D. Thesis, Caltech, ii+86 p.
- Bollay, W. (1939) "A Nonlinear Wing Theory and its Application to Rectangular Wings of Small Aspect Ratio." Zeit. angew. Math. Mech. (ZAMM), **19**(1):21–35.
- Brown, C. E. & W. H. Michael (1954) "Effect of leading edge separation on the lift of a delta wing." J. Aeronautical Science, **21**:690–706.
- Brown, C. E. & W. H. Michael, Jr. (1955) "On Slender Delta Wings with Leading-Edge Separation." National Advisory Committee for Aeronautics, Technical Note 8430, i+27 p.
- de Kat, J. O. (1994) "Irregular Waves and their Influence on Extreme Ship Motions," Proc. 20th Symp. Naval Hydro., Santa Barbara, CA, pp. 48–67.
- de Kat, J. O., R. Brouwer, K. A. McTaggart & W. L. Thomas, III (1994) "Intact Ship Survivability in Extreme Waves: New Criteria from a Research and Navy Perspective," Proc. 5th Int'l Conf. Stability of Ships and Ocean Vehicles (STAB 94), Florida Institute of Technology, Melbourne, FL, Vol. 1, 26 p.
- de Kat, J. O. & J. R. Paulling (1989) "The

- Simulation of Ship Motions and Capsizing in Severe Seas,” Trans. SNAME, **97**:139–168, Jersey City, NJ.
- DOD (1998) “DoD Modeling and Simulation (M&S) Glossary.” DoD 5000.59-M, U. S. Department of Defense.
- DOD (2003) “DoD Modeling and Simulation (M&S) Verification, Validation, and Accreditation (VV&A).” DoD Instruction 5000.61, U. S. Department of Defense.
- DOD (2007) “DoD Modeling and Simulation (M&S) Management.” DoD Directive 5000.59, U. S. Department of Defense.
- Dommermuth, D. G., T. T. O’Shea, D. C. Wyatt, T. Ratcliffe, G. D. Weymouth, K. L. Hendrikson, D. K. P. Yue, M. Sussman, P. Adams & M. Valenciano, (2007) “An Application of Cartesian-Grid and Volume-of-Fluid Methods to Numerical Ship Hydrodynamics.” Proc. 9th Int’l Conf. Numerical Ship Hydro., Ann Arbor, MI.
- Dommermuth, D. G., T. T. O’Shea, D. C. Wyatt, M. Sussman, G. D. Weymouth, D. K. P. Yue, P. Adams & R. Hand, (2006) “The Numerical Solution of Ship Waves Using Cartesian-Grid and Volume-of-Fluid Methods.” Proc. 26th Symp. Naval Hydro., Rome, Italy.
- Etebari, A., P. Atsavapranee, C. Bassler, and J. Carneal (2008) “Experimental Analysis of Rudder Contribution to Roll Damping,” Proc. 27th Int’l Conference on Offshore Mechanics and Arctic Engineering, OMAE 2008, Estoril, Portugal.
- Francescutto, A., G. Contento & R. Penna (1994) “Experimental Evidence of Strong Nonlinear Effects in the Rolling Motion of a Destroyer in Beam Seas”, Proc. 5th Int’l Conference of Stability of Ships and Ocean Vehicles (STAB 94), Florida Institute of Technology, Melbourne, FL, Vol. 1, 13 p.
- Fullerton, A. M., T. C. Fu & A. M. Reed (2008) “The Moments on a Tumblehome Hull Form Undergoing Forced Roll.” Proc. 27th Symp. on Naval Hydro., 12 p.
- Gersten, K. (1963) “A Nonlinear Lifting-Surface Theory Especially for Low-Aspect-Ratio Wings.” AIAA Journal, **1**:924–925.
- Gersten, K. (1961) “Nichtlineare Tragflächentheorie insbesondere für Tragflügel mit kleinem Seitenverhältnis.” Ingenieur-Archiv, **30**:431452.
- Grant, D. J., A. Etebari & P. Atsavapranee, (2007) “Experimental Investigation of Roll and Heave Excitation and Damping in Beam Wave Fields,” Proc. 26th Int’l Conference on Offshore Mechanics and Arctic Engineering, OMAE2007, San Diego, CA.
- Hayden, D. D., R. C. Bishop, J. T. Park & S. M. Lavery (2006) “Model 5514 Capsize Experiments Representing the Pre-Contract DDG 51 Hull Form at End of Service Life Conditions.” Carderock Division, Naval Surface Warfare Center Report NSWCCD-50-TR-2006/020, 82 p.
- Himeno, Y., 1981, “Prediction of Ship Roll Damping-State of the Art,” Dept. of Naval Architecture and Marine Engineering, Univ. of Michigan, Report 239.
- Howe, M. S. (1996) “Emendation of the Brown & Michael equation, with application to sound generation by vortex motion near a half-plane.” J. Fluid Mechanics, **329**:89101.
- Hughes, T. & D. Perrault (2008) “Critical Review of Naval Stability Standards.” Defence R&D Canada Report DRDC Atlantic ECR 2008-174, 38 p.
- Ikeda, Y., Y. Himeno, and N. Tanaka, 1978, “A Prediction Method for Ship Roll Damping,” Report of the Department of Naval Architecture, University of Osaka Prefecture, No. 00405.



- ITTC (2008) "The Specialist Committee on Stability in Waves: Final Report and Recommendations to the 25th ITTC." Proc. 25th ITTC, Fukuoko, Japan, 36 p.
- Kan, M. (1990) "Surging of large-amplitude and surf-riding of ships in following seas." Naval Architecture and Ocean Engineering, Society of Naval Architects of Japan, **28**:49–62.
- Kantz, H. & T. Schreiber (2004) "Nonlinear time series analysis." Cambridge University Press, Cambridge, UK, xvi+369 p.
- Kring, D. C., W. M. Milewski & N. E. Fine (2004) "Validation of a NURBS-Based BEM for Multihull Ship Seakeeping," Proc. 25th Symp. Naval Hydro., St. John's, Newfoundland and Labrador, Canada.
- Lighthill, M. J. (1960) "A Note on the Swimming of Slender Fish." J. Fluid Mech., **9**:305–17.
- Liut, D. A., K. W. Weems & W.-M. Lin (2002) "Nonlinear Green Water Effects On Ship Motions and Structural Loads." Proc. 24th Symp. on Naval Hydro., Fukuoka, Japan.
- Longuet-Higgins, M. S. (1957) "The statistical analysis of a random, moving surface." Phil. Trans. Roy. Soc., A **249**:32187.
- McCue, L. S., W. R. Story & A. M. Reed (2008) "Nonlinear Dynamics Applied to the Validation of Computational Methods." Proc. 27th Symp. on Naval Hydro., 10 p, Seoul, South Korea.
- McTaggart, K. A. & J. O. de Kat (2000) "Capsize risk of intact frigates in irregular seas." Trans. SNAME, **108**:147–77.
- McTaggart, K. A. (2000) "Ship capsize risk in a seaway using fitted distributions to roll maxima." J. Offshore Mechanics and Arctic Engineering, **122**:141–146.
- Miller, R. W., C. C. Bassler, P. Atsavapranee, and J. J. Gorski (2008) "Viscous Roll Predictions for Naval Surface Ships Appended with Bilge Keels Using URANS," Proc. 27th Symp. on Naval Hydro., Seoul, South Korea.
- NATO (2007a) "Buoyancy, Stability and Controllability." Chapter III of Naval Ship Code, NATO Naval Armaments Group, Maritime Capability Group 6, Specialist Team on Naval Ship Safety and Classification, Allied Naval Engineering Publication ANEP – 77, vii+121 p.
- NATO (2007b) "Guidance on NSC Chapter III Buoyancy and Stability, Part B: Application." Chapter 3, Guide to the Naval Ship Code, NATO Naval Armaments Group, Maritime Capability Group 6, Specialist Team on Naval Ship Safety and Classification, 91 p.
- Newman, J. N. (1975) "Swimming of slender fish in a non-uniform velocity field." J. Australian Mathematical Society, Series B, Applied Mathematics, **19**(1):95–111.
- Newman, J. N. & T. Y. Wu (1974) "Hydromechanical aspects of fish swimming." in Swimming and Flying in Nature, T. Y. Wu, C. J. Brokaw & C. J. Brennan, Editors; Plenum Press, Vol. 2, pp. 615–634.
- Rahola, J. (1939) "The judging of the stability of ships and the determination of the minimum amount of stability especially considering the vessel navigating Finnish waters." PhD Thesis, Technical University of Finland, Helsinki, viii+232 p.
- Reed, A. M. (2008) "Discussion of: Belenky, V. L., J. O. de Kat & N. Umeda (2008a)." Marine Tech., **45**(2):122–123.
- Rudgley, G., E. C. A. ter Bekke, P. Boxall, R. Humphrey (2005) "Development of a NATO 'Naval Ship Code'." RINA Conference on Safety Regulations and Naval Class

- II, RINA, London, United Kingdom, 8 p.
- Sarchin, T. H. & L. L. Goldberg (1962) "Stability and buoyancy criteria for U. S. Naval surface ships." Trans. SNAME, **72**:418–58.
- Spyrou, K. J. (2006) "Dynamic Instability in Quartering Seas: The Behavior of a Ship During Broaching." J. Ship Research, 40(1):4659.
- Spyrou, K. J. (2007) "Dynamic Instability in Quartering Seas—Part III: Nonlinear Effectson Periodic Motions." J. Ship Research, 41(3):210223.
- Spyrou, K. J., K. M. Weems, V. Belenky (2009) "Patterns of Surf-Riding and Broaching-to Captured by Advanced Hydrodynamic Modelling." Proc. 10th Int'l Conf. Stability of Ships and Ocean Vehicles (STAB 09), St. Petersburg, Russia, 15 p.
- Telste, J. G. & W. F. Belknap (2008) "Potential Flow Forces and Moments from Selected Ship Flow Codes in a Set of Numerical Experiments." Carderock Division, Naval Surface Warfare Center Report NSWCCD-50-TR–2008/040, 15,240 p.
- Themelis, N. & K. J. Spyrou (2007) "Probabilistic Assessment of Ship Stability," Trans. SNAME, **115**:181–206.
- Themelis, N. & K. J. Spyrou (2008) "Probabilistic Assessment of Ship Stability Based on the Concept of Critical Wave Groups," Proc. 10th Int'l Ship Stability Workshop, Daejeon, Korea.
- US Navy (2003) "Stability and buoyancy of U.S. Naval surface ships." Design Data Sheet DDS 079-1, Version 1.21, 81 p.
- van Zwol, J. A. (2004) "Design aspects of submerged vanes." M. Sc. Thesis, Delft University of Technology, Delft, The Netherlands, 126 p.
- Wheeler, J. D. (1969) "Method of calculating forces produced by irregular waves." Proc. Offshore Technology Conference (OTC 1006), Vol. 1, pp. 71–82, Houston, TX.

